Original Article

JCBFM

Journal of Cerebral Blood Flow & Metabolism
2018, Vol. 38(10) 1754–1768

DOI: 10.1177/0271678X17714680
journals.sagepub.com/home/jcbfm
SAGE

Glutamate dehydrogenase is essential to sustain neuronal oxidative energy metabolism during stimulation

Michaela C Hohnholt[1], Vibe H Andersen[1], Jens V Andersen[1], Sofie K Christensen[1], Melis Karaca[2], Pierre Maechler[2] and Helle S Waagepetersen[1]

Abstract

The enzyme glutamate dehydrogenase (GDH; Glud1) catalyzes the (reversible) oxidative deamination of glutamate to α-ketoglutarate accompanied by a reduction of NAD^+ to NADH. GDH connects amino acid, carbohydrate, neurotransmitter and oxidative energy metabolism. Glutamine is a neurotransmitter precursor used by neurons to sustain the pool of glutamate, but glutamine is also vividly oxidized for support of energy metabolism. This study investigates the role of GDH in neuronal metabolism by employing the Cns-*Glud1*$^{-/-}$ mouse, lacking GDH in the brain (GDH KO) and metabolic mapping using ^{13}C-labelled glutamine and glucose. We observed a severely reduced oxidative glutamine metabolism during glucose deprivation in synaptosomes and cultured neurons not expressing GDH. In contrast, in the presence of glucose, glutamine metabolism was not affected by the lack of GDH expression. Respiration fuelled by glutamate was significantly lower in brain mitochondria from GDH KO mice and synaptosomes were not able to increase their respiration upon an elevated energy demand. The role of GDH for metabolism of glutamine and the respiratory capacity underscore the importance of GDH for neurons particularly during an elevated energy demand, and it may reflect the large allosteric activation of GDH by ADP.

Keywords

Mitochondria, glutamine, neurons, respiration, GDH

Received 23 December 2016; Accepted 9 May 2017

Introduction

Glutamate is the main excitatory neurotransmitter in the brain[1] and glutamate dehydrogenase (GDH) is an equilibrium enzyme which catalyzes both the oxidative deamination of glutamate to α-ketoglutarate as well as reductive amination in the reverse direction. Dysregulation of glutamate homeostasis[2] and of GDH have been suggested to play a role in several neurodegenerative diseases. In the brain, GDH is expressed in astrocytes and neurons,[3,4] but little is known so far about the significance of GDH in neuronal metabolism and energy generation. Metabolically, the oxidative deamination of glutamate to α-ketoglutarate is able to replenish the pool of tricarboxylic acid (TCA) cycle intermediates, that is anaplerosis. The most abundant aminotransferase in brain,[5] aspartate aminotransferase (AAT) also catalyzes the formation of α-ketoglutarate from glutamate by transferring the amino group to oxaloacetate, generating aspartate without increasing the total pool of TCA cycle intermediates.[6]

In astrocytes, partial reduction of GDH activity resulted in an up-regulation of AAT and net formation

[1]Department of Drug Design and Pharmacology, Faculty of Health and Medical Science, University of Copenhagen, Copenhagen, Denmark
[2]Department of Cell Physiology and Metabolism, CMU, University of Geneva, Geneva, Switzerland

Corresponding authors:
Michaela C Hohnholt, Department of Drug Design and Pharmacology, Faculty of Health and Medical Science, University of Copenhagen, Universitetsparken 2, 2100 Copenhagen, Denmark.
Email: hohnholt@uni-bremen.de
Helle S Waagepetersen, Department of Drug Design and Pharmacology, Faculty of Health and Medical Science, University of Copenhagen, Universitetsparken 2, 2100 Copenhagen, Denmark.
Email: helle.waagepetersen@sund.ku.dk

of aspartate via the truncated TCA cycle,[7] a higher dependency on glucose metabolism[8] and an up-regulation of anaplerotic reactions.[9] In the Cns-*Glud1*$^{-/-}$ mouse, not expressing GDH (GDH KO), brain glutamine levels were increased and oxidative glutamate catabolism in the brain[10] and in astrocytes was decreased.[11]

Neurons exhibit a high specific activity of GDH[12] and GDH activity is altered by the cellular energy level due to the allosteric activation by ADP.[3] Glutamine is important for neurons as precursor for glutamate synthesis to sustain glutamatergic neurotransmission but also as a substrate for the replenishment of TCA cycle intermediates.[13,14] The entrance of glutamine-derived carbon into the TCA cycle is very active[15]and depends on GDH[16] in synaptosomes. Furthermore, synaptosomes use glutamine as substrate for the truncated TCA cycle to generate energy in the absence of glucose.[15,17]

To investigate the physiological role of GDH in neuronal metabolism and its contribution during stimulation, we used metabolic mapping employing [U-^{13}C]glutamine[18,19] as neuronal substrate in acutely isolated synaptosomes and cultured cerebellar neurons obtained from control or GDH KO mice. Because astrocytes, exhibiting reduced GDH activity, are more dependent on glucose metabolism,[8] we also investigated if glucose metabolism is altered in the absence of GDH using [U-^{13}C]glucose in our models of neurons not expressing GDH.

In summary, we show that GDH is a crucial enzyme for neurons to metabolize glutamine-derived carbon in the TCA cycle during glucose deprivation. In contrast to the findings in astrocytes, the experimentally induced lack of GDH activity in neurons does not affect glucose metabolism under basal conditions. In addition, GDH plays an important role in neurons in order to increase respiration in case of a sudden elevated energy demand experimentally induced by veratridine or uncoupling. Additionally, mitochondrial respiration in the presence of glutamate as substrate is GDH-dependent.

Materials and methods

Materials

D-Glucose-$^{13}C_6$ ([U-^{13}C]glucose) and L-glutamine-$^{13}C_6$ ([U-^{13}C]glutamine) (both 99% enrichment) were obtained from Cambridge Isotope Laboratories (Andover, USA). All other chemicals of the purest grade available were from regular commercial sources.

Brain-specific GDH knockout mouse Cns-Glud1 −/−

Cns-*Glud1*$^{-/-}$ mice and control (*Glud*$^{lox/lox}$) mice[11,20] were bred at the Department for Drug Design and Pharmacology (University of Copenhagen, Denmark) in a temperature controlled environment (12 h/12 h light/dark cycle, free access to water/standard chow). Both male and female mice were used. Mice were handled according to standards given by the Danish Animal Experiments Inspectorate. The experiments were approved by the Danish National Ethics Committee, performed according to the European Convention (ETS 123 of 1986) and reported according to ARRIVE guidelines.

Mitochondrial isolation

A mouse was sacrificed by cervical dislocation. The whole brain was excised and placed in a 15 mL Teflon/glass (Wheaton, USA) homogenizer containing ice-cold homogenizing buffer (in mM: 100 KCl, 50 Tris, 5 $MgCl_2$, 1.8 ATP, 1 EDTA, pH 7.2) corresponding to 50 mg tissue/mL. The brain was homogenized (100 r/min, 3 min) and the homogenate was centrifuged (650 g, 3 min, 4°C, Beckman Coulter, JA-20). The supernatant was centrifuged (15,000 g, 3 min, 4°C) and the supernatant was discarded. The pellet was washed with homogenization buffer and centrifuged (15,000 g, 3 min, 4°C). The supernatant was again discarded and the pellet was resuspended in suspension buffer (mM: 200 sucrose, 15 K_2HPO_4, 2 $MgSO_4$, 0.5 EDTA, 0.5 mg/mL BSA, pH 7.2) corresponding to 20% of the original homogenization buffer. This re-suspension contained the isolated pre- and post-synaptic mitochondria from both neurons and glial cells.

Isolation of nerve terminal endings and cerebellar neuron cultures

Isolation of nerve terminal endings from mice was performed according to a recently published method.[21] Cerebellar neurons were isolated and cultured from 7-day-old mice as described before.[22] Briefly, the cerebellum was excised, subsequently trypsinized with 0.25 mg/mL trypsin for 15 min at 37°C. Trypsin was inactivated by trypsin inhibitor (0.53 mg/mL) and the tissue was subsequently triturated. The obtained cells were seeded on poly-D-lysin-coated dishes in modified Dulbecco's medium containing 24.5 mM KCl, 12 mM glucose, 7 μM p-aminobenzoate, 50 μM kainate and 10% (v/v) fetal calf serum. Astrocyte proliferation was prevented by addition of 20 μM cytosine arabinoside after 48 h in culture. The cultures were kept in an incubator at 37°C in a humidified atmosphere containing 5% CO_2. A minimum concentration of 12 mM glucose was ensured by supplementing glucose twice until the cultures were used at day 7–8 in vitro. The cultures contained 80–90% neurons with glutamatergic phenotype and 5–10% glial cells.[23]

Protein determination

The protein content of the synaptosomes was determined directly after the isolation by the Bradford protein assay (Sigma–Aldrich, St. Louis, USA) and 0.3–0.5 mg of synaptosomal protein was used per condition for incubation. The protein contents of cerebellar neurons and synaptosomes were determined after the incubations by the Lowry protein determination[24] and these protein contents after the incubations were used to normalize the amino acid contents. Bovine serum albumin (BSA) was used as a standard.

Western blots

Proteins were denatured by boiling the sample (5 min) in NuPAGE® LDS Sample Buffer (ThermoFisher Scientific, Carlsbad, CA, USA) with 50 mM DTT. Ten micrograms of protein per lane was resolved on a 4–12% Bis–Tris pre-cast gel using the XCell SureLockTM mini-electrophoresis system (ThermoFisher). Proteins were transferred onto a PVDF membrane with constant 30 V for 2 h in NuPAGE® Transfer Buffer (ThermoFisher) with 20% methanol. The membranes were blocked for 1.5 h at room temperature (RT) in 2% (w/v) non-fat skim milk protein and 0.1% Tween-20 in wash buffer (mM: 50 Tris base, 100 NaCl, pH 7.2). The membranes were incubated overnight at 4°C with Abcam antibodies of GDH (ab34786, 1:1000), AAT (ab93928, 1:2000) or β-actin (ab8227, 1:2000). After three washes (5 min each), the membranes were incubated (1.5 h, RT) with appropriate HRP-conjugated secondary antibodies (Dako, Glostrup, Denmark). All antibodies were diluted in washing buffer with 0.2% (w/v) non-fat skim milk and 0.05% Tween-20. The bands were visualized using ECL™ Prime Western Blotting Detection Reagent (GE Healthcare, Buckinghamshire, UK).

GDH and AAT activity assay

GDH and AAT activity assays were performed for isolated mitochondria from GDH KO mice or control mice. The mitochondrial suspension (500 µL) was homogenized (100 r/min, 2 min) in a 15 mL Teflon/glass homogenizer with 1% Triton X (final concentration) and afterwards incubated on ice for 30 min. After centrifugation (8000 g, 10 min, 4°C), the supernatant containing the enzyme(s) was used for GDH and AAT activity determination in a 96-well plate using a spectrophotometer at RT by following the reaction as a decline in absorbance at 340 nm for 10 min (300 µL/well total volume).

The GDH activity assay was performed in a buffer (mM: 50 triethanolamine, 2.6 EDTA, 100 ammonium acetate, pH 8.0) and 0.1 mM NADPH was added corresponding to an absorbance of 0.433. Enzyme solution (10 µL) was added together with 1 mM ADP and 8 mM α-ketoglutarate (final concentrations) to start the reaction.

AAT activity was determined coupled to malate dehydrogenase (MDH) activity. It was performed in a buffer (0.1 M Tris–HCl, 0.02 mM pyridoxal 5-phosphate, 20 mM L-aspartate, pH 7.2). Purified MDH (4 U/mg protein) and 0.15 mM NADH were added (final concentrations). Afterwards 10 µL enzyme was added, and the 96-well plate was incubated for 10 min at RT (until stabile absorbance). α-Ketoglutarate (2.5 mM final concentration) the immediate substrate for AAT was added to initiate the reaction. Specific enzyme activity (SA) was calculated using the equation (modified Lambert Beer's law) below

$$SA\,(\mu\text{mol}/(\text{min}*\text{mg})) = \frac{\frac{\left(\frac{dAbs}{\text{min}}\right)}{\mu L\,\text{enzyme}} * 300\,\mu\text{L}}{\left(\frac{6.22}{\text{mM}*\text{cm}}\right) * \text{protein}\left(\frac{\text{mg}}{\text{mL}}\right) * 0.7\,\text{cm}}$$

(300 µL volume, molar extinction coefficient NAD(P)H: 6.22 $mM^{-1}cm^{-1}$, 0.7 cm light path through a well of a 96-well plate).

Mitochondrial respiration

Respiration of isolated mitochondria was measured by the Seahorse XF^e96 flux analyzer (Seahorse Biosciences, MA, USA). Briefly, the plate containing 4 µg mitochondria/well in 25 µL mitochondrial assay buffer (MAS; mM: 70 sucrose, 220 mannitol, 10 KH_2PO_4, 5 $MgCl_2$, 2 HEPES and 0.2% BSA (fatty acid free), pH 7.2) was centrifuged (2000*g*, 20 min, 4°C) and 155 µL prewarmed 37°C MAS containing (in mM) 10 pyruvate and 2 malate or 10 glutamate and 10 malate (all final concentrations). After calibration of the cartridge, the mitochondria plate was inserted. After 10 min waiting, two cycles (1 min mixing, 3 min waiting time) were employed, followed by three cycles (2 min mixing, 1 min waiting, 3 min measurement). Before each injection, 2 min mixing and 1 min waiting, followed by injection of the indicated compound, followed by 1 min waiting and 3 min measurement was performed. At the indicated time points, final concentrations of 4 mM ADP, 2.5 µg/mL oligomycin A, 8 µM FCCP and 8 µM antimycin A were added. Oxygen consumption rates (OCR; pmol/min) were calculated by the Wave software (Seahorse Bioscience).

Incubation studies using ^{13}C-labelled substrates

Synaptosomes were incubated in medium (Dulbecco's minimum essential medium without fetal calf serum pH

7.4 (DMEM)) containing 0.5 mM [U-^{13}C]glutamine ± 2.5 mM unlabelled D-glucose or 2.5 mM [U-^{13}C]glucose for 45 min at 37°C. After the incubation, synaptosomes were centrifuged (1000*g*, 2 min, 4°C), washed once with phosphate buffered saline (PBS; in mM: 137 NaCl, 2.7 KCl, 7.3 Na_2HPO_4, 1.5 KH_2PO4, 0.9 $CaCl_2$, 0.5 $MgCl_2$), subsequently extracted with 70% ice-cold ethanol, lyophilized and stored (−20°C) until further analysis by gas chromatography-mass spectrometry (GC-MS) and high-performance liquid chromatography (HPLC).

Cultures of cerebellar neurons were washed once with 37°C medium (DMEM) and subsequently incubated in medium containing 0.5 mM [U-^{13}C]glutamine or 2.5 mM [U-^{13}C]glucose for 2 h at 37°C. After the incubation, the medium was collected, the cells were washed once with ice-cold PBS, extracted with 70% ice-cold ethanol, lyophilized and stored (−20°C) until further analysis.

After ethanol extraction of synaptosomes or neurons, the remaining protein pellet was dried and reconstituted in 1 M KOH for protein determination.

Metabolic mapping of metabolites of interest by GC-MS and HPLC

Dried extracts of cerebellar neurons or synaptosomes were re-suspended in 150 µL or 200 µL H_2O, respectively, and used for GC-MS analysis as described before.[23,25] Using unlabelled standards, the isotope enrichment of the metabolites was calculated and corrected for natural abundance of ^{13}C. Each isotopomer M + X (M = mass of the unlabelled molecule, X = number of ^{13}C labelled carbon atoms) is presented as percent of the total pool of the metabolite. An overview of the metabolite labelling patterns expected after metabolism of the different substrates are shown in Figure 2(b) and (d) and Figure 4(a). The labelling derived from metabolism of [U-^{13}C]glucose in the TCA cycle is depicted in Figure 4(a). Condensation of oxaloacetate M + 2 with acetyl (M + 2)-CoA increases the number of ^{13}C in the products (e.g. citrate M + 4, α-ketoglutarate M + 3/M + 4, succinate M + 3, fumarate M + 3, malate M + 3, aspartate M + 4 and glutamate M + 3/M + 4). The calculated cycling ratio is a measure of TCA cycle activity as described previously.[26]

Amino acid contents in cell extracts were determined by reversed-phase HPLC as described before.[25]

Seahorse Bioscience XFe96 extracellular flux analyzer

Synaptosomal respiration was investigated as described previously.[21] OCR and extracellular acidification rates (ECAR) were calculated using the Wave software. From the mean of two OCR values, the following respiration parameters were calculated

$$\mathrm{OCR}_{(\text{basal respiration})} = \mathrm{OCR}_{(\text{initial respiration})} - \mathrm{OCR}_{(\text{rotenone/antimycinA})}$$

$$\mathrm{OCR}_{(\text{maximal respiration})} = \mathrm{OCR}_{(\text{FCCP})} - \mathrm{OCR}_{(\text{rotenone/antimycinA})}$$

$$\mathrm{OCR}_{(\text{spare respiratory capacity})} = \mathrm{OCR}_{(\text{FCCP})} - \mathrm{OCR}_{(\text{basal respiration})}$$

Presentation of data

The data shown represent means ± SEM of values that were obtained in experiments performed on independent batches of cultured cerebellar neurons, synaptosomal or mitochondrial preparations. Significance of differences between the values obtained for control synaptosomes/neurons/mitochondria compared to GDH KO synaptosomes/neurons/mitochondria were calculated by the Students' *t*-test ($^*p < 0.05$, $^{**}p < 0.01$ and $^{***}p < 0.001$; Figures 1 to 5). Significance of differences between values obtained for control synaptosomes compared to GDH KO synaptosomes were calculated by two-way ANOVA ($^*p < 0.05$, $^{**}p < 0.01$ and $^{***}p < 0.001$; Figure 6). $p > 0.05$ was considered as not statistically significant.

Results

Enzyme expression, enzyme activity and respiration of isolated mitochondria

Brain mitochondria from control mice expressed GDH (control mitochondria), while brain mitochondria from Cns-*Glud1*$^{-/-}$ mice (GDH KO mitochondria) did not express GDH (Figure 1(a)). No differences in the expression level of AAT from control and GDH KO mitochondria were observed (Figure 1(a)). The enzyme activity of GDH followed Michaelis–Menten kinetics in control mitochondria ($K_m = 1.752$ mM, $V_{max} = 0.1577$ µmol/(min × mg)),[27] while in GDH KO mitochondria no GDH activity was observed (Figure 1(b)). The activity of AAT was not different in GDH KO ($K_m = 0.6859$ mM, $V_{max} = 0.3257$ µmol/(min × mg)) compared to control mitochondria ($K_m = 0.2901$ mM, $V_{max} = 0.3553$ µmol/(min × mg)) in the presence of α-ketoglutarate as substrate (Figure 1(b)). Independent of GDH activity, ADP induces respiration of mitochondria in the presence of pyruvate + malate (Figure 1(c) and (d)). However, in the presence of glutamate + malate the mitochondria

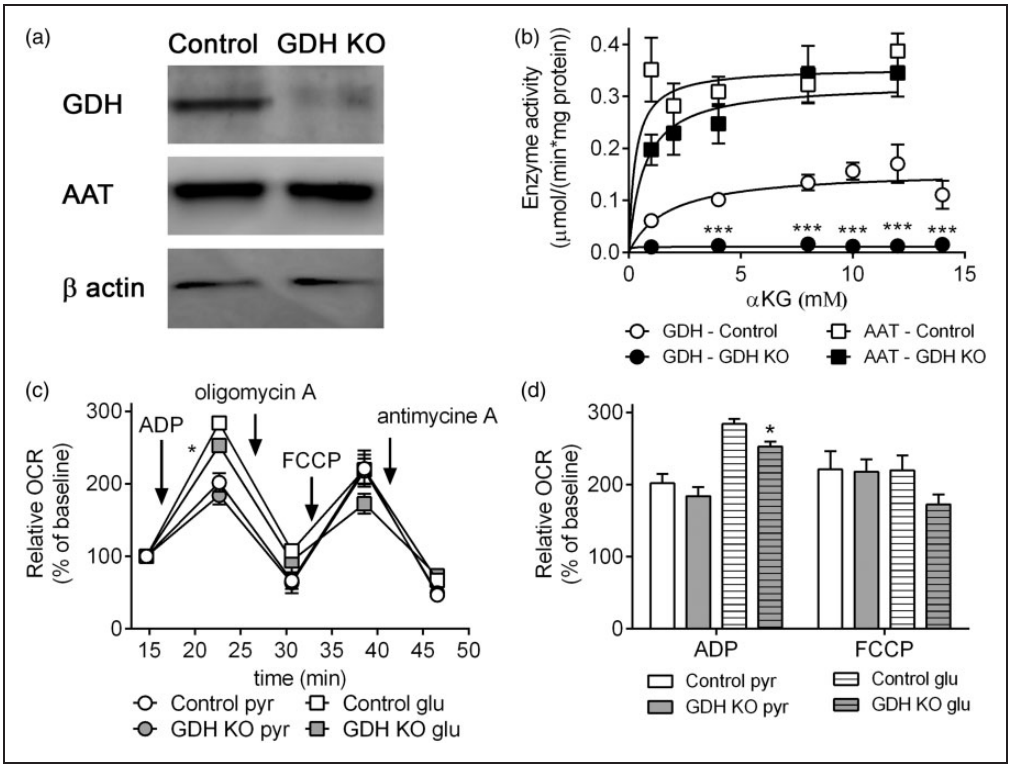

Figure 1. Expression and enzyme activity of GDH and AAT and respiration of isolated brain mitochondria. The expression of GDH and AAT determined by Western blot (loading control: β-actin) (a) and enzyme activities of GDH and AAT (b) in mitochondria from control (white) and GDH KO mice (black). The respiration of mitochondria from control (white) and GDH KO mice (gray) was measured in the presence of pyruvate + malate or glutamate + malate as substrates (c, d). The relative change of OCR was calculated by normalization of the 3rd basal measurements to 100% (control: 72.3 ± 17.4 pmol/min; GDH KO: 61.9 ± 10.6 pmol/min with pyruvate + malate; control: 57.6 ± 12.8 pmol/min, GDH KO: 45.8 ± 8.3 pmol/min with glutamate + malate) (c, d). The data shown are mean ± SEM of values obtained on 3 independent mitochondria preparations (each preparation and condition: 13–15 wells/experiment).

lacking GDH respired significantly lower compared to control mitochondria (Figure 1(d)). The oxygen consumption, which is independent of ATP synthesis and the maximal respiration induced by FCCP, were not different in GDH KO mitochondria compared to control mitochondria (Figure 1(c) and (d)).

Hampered glutamine metabolism in GDH KO synaptosomes

Synaptosomes isolated from brains of control mice (control synaptosomes) and Cns-*Glud1*$^{-/-}$ mice (GDH KO synaptosomes) were incubated in the presence of [U-^{13}C]glutamine (i.e. glutamine M + 5) to investigate the role of GDH in oxidative metabolism of glutamine in the absence of glucose. The total amount of glutamine and glutamine M + 5 were not different in control compared to GDH KO synaptosomes (Figure 2(a)) and comparable to literature[15] values suggesting that plasma membrane uptake of glutamine is not affected by the lack of GDH activity.

The labelling derived from [U-^{13}C]glutamine by direct TCA cycle metabolism is presented in Figure 2(b). The percent ^{13}C glutamine (M + 5) and glutamate M + 5 from [U-^{13}C]glutamine taken up and metabolized by phosphate-activated glutaminase was not different in control and GDH KO synaptosomes. However, α-ketoglutarate M + 5, the first TCA cycle intermediate, is not differently labelled in GDH KO synaptosomes compared to control (Figure 2(c)). The labelling of all further TCA cycle intermediates investigated was reduced and for succinate M + 4, fumarate M + 4 and the oxaloacetate-derived amino acid aspartate M + 4, the decrease was significant (Figure 2(c)). The labelling patterns of metabolites formed in the first turn of TCA cycle metabolism after [U-^{13}C]glutamine metabolism to citrate M + 4 are depicted in Figure 2(d). The percent ^{13}C labelling of all TCA cycle intermediates, glutamate and aspartate were significantly reduced (exception: malate M + 2 and citrate M + 2; Figure 2(e). The percent ^{13}C labelling is dependent on pool sizes (nmol/mg protein) and the amount of ^{13}C

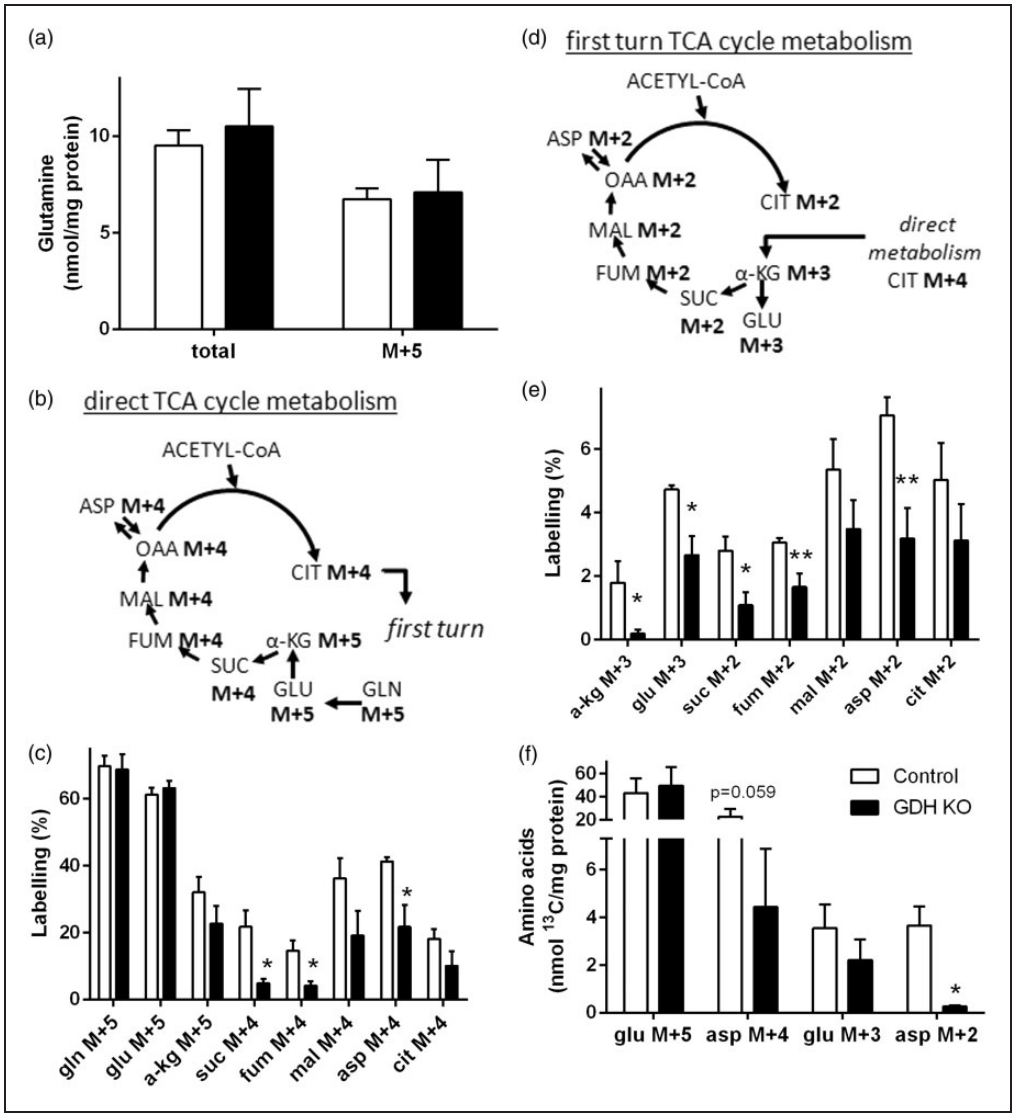

Figure 2. Metabolism of [U-^{13}C]glutamine in GDH KO synaptosomes. Synaptosomes were isolated from control (white) and GDH KO mice (black) and incubated with [U-^{13}C]glutamine. The synaptosomal extracts were analyzed for amino acid contents by HPLC and for percentage ^{13}C labelling by GC-MS (a, c, e, f). The labelling patterns derived from [U-^{13}C]glutamine (M + 5) after conversion to glutamate M + 5 and subsequent entrance into the TCA cycle by direct (b) and after first turn TCA cycle (d) metabolism that corresponds to the data shown in (c) and (e), respectively. Direct metabolism of [U-^{13}C]glutamine (M + 5) leads to formation of citrate M + 4 (b), which can be further metabolism during the first turn of the TCA cycle (d). The legend in (f) applies to all panels. Asp, aspartate; cit: citrate; fum, fumarate; gln, glutamine; glu, glutamate; mal, malate; suc, succinate; α-kg, α-ketoglutarate. ($n = 4$–7 independently prepared synaptosomes per condition.)

incorporated. Therefore, the amounts of labelled glutamate and aspartate (nmol ^{13}C/mg protein) were calculated (Figure 2(f)). No differences in the amount of glutamate M + 5 and glutamate M + 3 were observed, whereas the amounts of aspartate M + 4 and aspartate M + 2 were lower in the absence compared to the presence of GDH (Figure 2(f)). As mentioned above, the uptake of glutamine in synaptosomes seems not to be lower by the absence of GDH, thus, the changes observed in glutamine metabolism occur downstream in the oxidative metabolism of glutamine.

Hampered glutamine metabolism in GDH KO neurons

To test if the changes in [U-^{13}C]glutamine metabolism are a feature of GDH in synaptosomal metabolism or reflect metabolic changes of whole neurons,

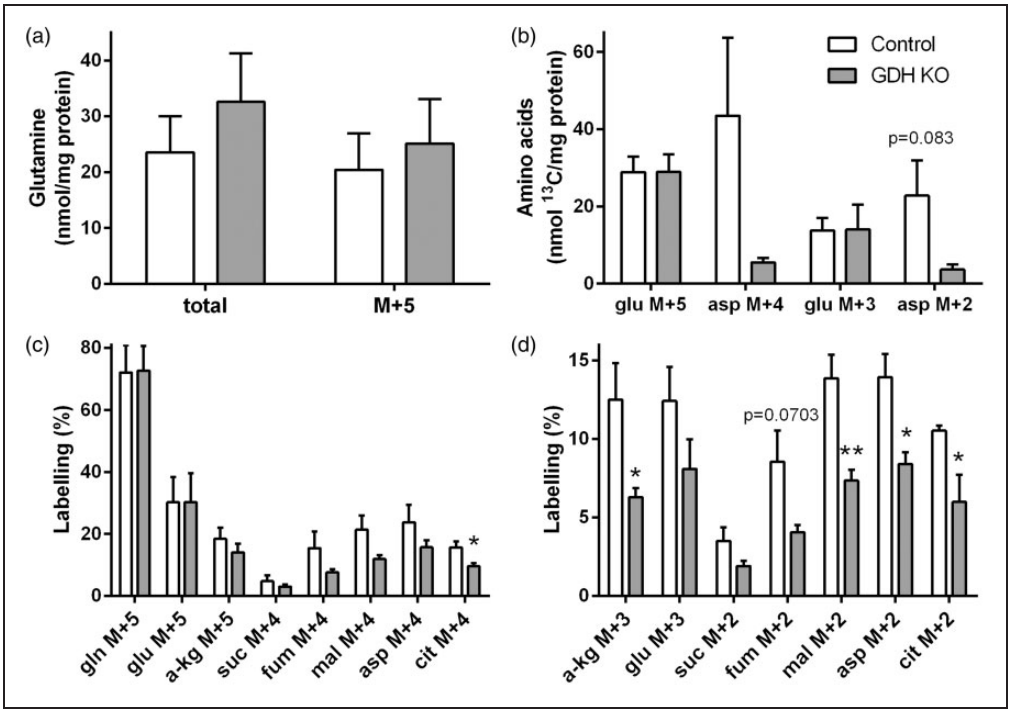

Figure 3. Metabolism of [U-^{13}C]glutamine in GDH KO neurons. Control (white) and GDH KO (grey) neurons were incubated with [U-^{13}C]glutamine and the cell extracts were analyzed for amino acid contents by HPLC (a, b) and for percent ^{13}C labelling by GC-MS (a, c, d). (b) Amounts of ^{13}C labelling (nmol ^{13}C/mg protein) glutamate M + 5 and M + 3 and aspartate M + 4 and M + 2 are presented. The labelling patterns derived from [U-^{13}C]glutamine (M + 5) after conversion to glutamate M + 5 and subsequent entrance into the TCA cycle by direct labelling are as shown in Figure 2(b) and (d). The legend in (b) applies to all panels. Asp, aspartate; cit: citrate; fum, fumarate; gln, glutamine; glu, glutamate; mal, malate; suc, succinate; α-kg, α-ketoglutarate. ($n = 3$–5 independently prepared neuron cultures per condition.)

[U-^{13}C]glutamine metabolism was also investigated in cultured glutamatergic neurons obtained from Cns-*Glud1*$^{-/-}$ mice (GDH KO) and control mice. The expected labelling patterns are the same as shown in Figure 2(b) and (d). No differences in the cellular content of glutamine and in the amount of labelled glutamine M + 5 were observed in GDH KO neurons (Figure 3(a)), as observed in the synaptosomal model system. The amounts of glutamate M + 5 and glutamate M + 3 were not different from control, whereas no significant differences in the amounts of aspartate M + 4 and aspartate M + 2 were observed in GDH KO neurons (Figure 3(b)). The percent labelling of glutamine M + 5, glutamate M + 5, α-ketoglutarate M + 5 and the TCA cycle intermediates directly obtained from [U-^{13}C]glutamine showed a trend towards less labelling in GDH KO neurons compared to control neurons and citrate M + 4 was significantly decreased (Figure 3(c)). Thus, the effect of GDH is similar to that seen in synaptosomes. In line with this, the labelling of α-ketoglutarate M + 3, malate M + 3, aspartate M + 3 and citrate M + 2 obtained from [U-^{13}C]glutamine in the first turn of TCA cycle metabolism was significantly lower in GDH KO neurons in (Figure 3(d)).

Glucose metabolism is not affected by the absence of GDH in synaptosomes or cultured neurons

Glutamine contributes via glutamate to anaplerosis (synthesis of TCA cycle intermediates for replenishment of TCA cycle intermediates), and thereby increase the capacity of the TCA cycle to oxidize acetyl-CoA formed from glucose. In order to evaluate the effect of GDH on glucose metabolism, synaptosomes and cultured neurons were incubated in medium containing [U-^{13}C]glucose. The labelling patterns derived from [U-^{13}C]glucose are shown for first turn TCA cycle metabolism (Figure 4(a), for further labelling patterns see methods). A trend towards higher labelling was observed in lactate M + 3 of GDH KO synaptosomes and GDH KO cultured neurons (Figure 4(b)). No differences were observed in the labelling of alanine M + 3 in GDH KO synaptosomes (control: 11.9% ± 3.2%; GDH KO: 15.7% ± 3.2%) or neurons

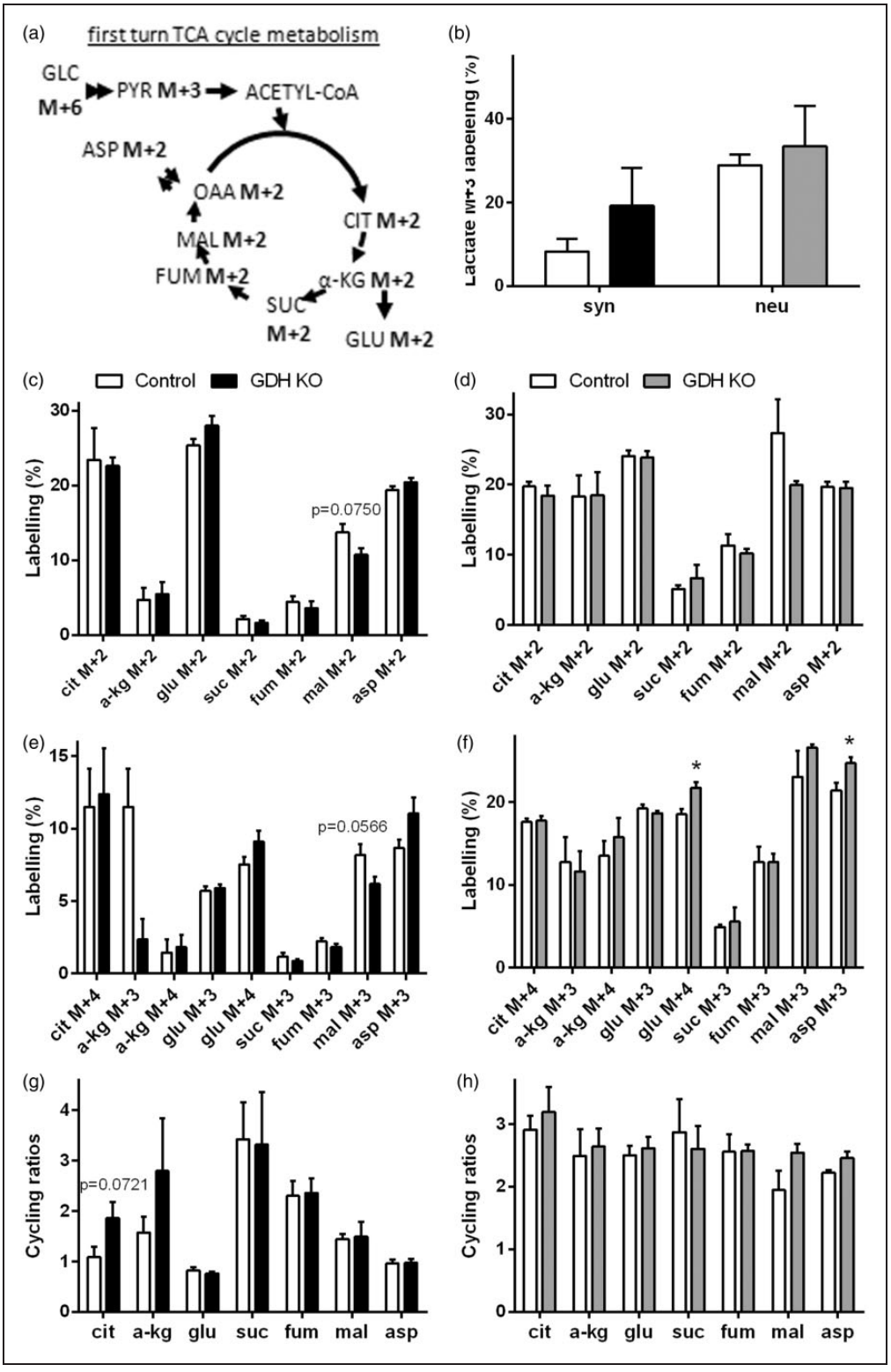

Figure 4. Metabolism of [U-^{13}C]glucose in GDH KO synaptosomes and GDH KO neurons. The labelling patterns derived from [U-^{13}C]glucose (M + 6) after conversion to pyruvate M + 3 and subsequent entrance of labelling into the TCA cycle (a). Control synaptosomes (white, b, c, e, g) or neurons (white, b, d, f, h) and GDH KO synaptosomes (black, b, c, e, g) or GDH KO neurons (gray, b, d, f, h) were incubated with [U-^{13}C]glucose and extracts were analyzed by GC-MS for ^{13}C labelling derived from metabolism of [U-^{13}C]glucose (b-f). Cycling ratios, indicating TCA cycle activity, are calculated by dividing labelling from subsequent TCA cycle turns by that from first turn, in synaptosomes (g) and cultured neurons (h). Ala, alanine; asp, aspartate; cit: citrate; fum, fumarate; glu, glutamate; mal, malate; pyr, pyruvate suc, succinate; α-kg, α-ketoglutarate. ($n = 4$–6 independently prepared synaptosome preparations or three independently prepared neuron cultures per condition.)

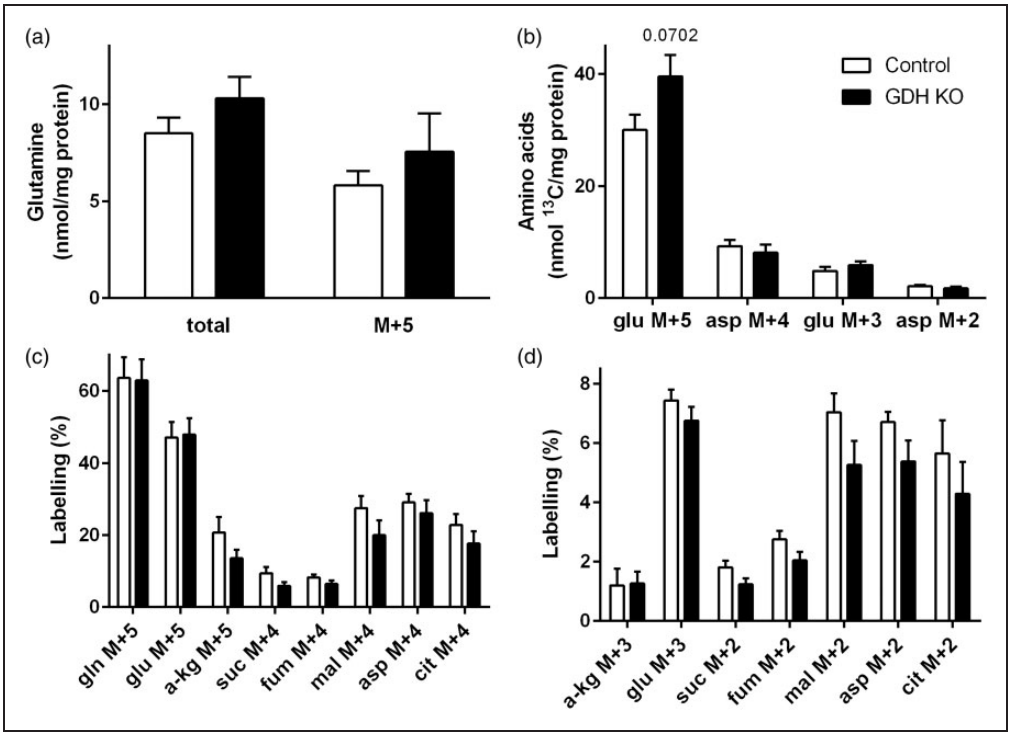

Figure 5. Metabolism of [U-^{13}C]glutamine in the presence of unlabelled glucose in GDH KO synaptosomes. Control (white) and GDH KO (black) synaptosomes were incubated with [U-^{13}C]glutamine with unlabelled glucose and the synaptosomal extracts were analyzed for amino acid contents by HPLC (a, b) and for percentage ^{13}C labelling by GC-MS (c, d). The labelling patterns derived from [U-^{13}C]glutamine (M + 5) after conversion to glutamate M + 5 and subsequent entrance into the TCA cycle by direct labelling are as shown in Figure 2(b) and (d). The legend in (b) applies to all panels. Asp, aspartate; cit: citrate; fum, fumarate; gln, glutamine; glu, glutamate; mal, malate; suc, succinate; α-kg, α-ketoglutarate. ($n = 5$–8 independently prepared synaptosome preparations per condition.)

(control: 21.2% ± 6.5%; GDH KO: 32.0% ± 9.9%). ^{13}C Enrichment of all TCA cycle intermediates, glutamate and aspartate derived in the first turn of the TCA cycle, were not affected by the absence of GDH in synaptosomes (Figure 4(c)) or cultured neurons (Figure 4(d)). Likewise, in the second turn of the TCA cycle, metabolizing another [1,2-^{13}C]acetyl-CoA derived from [U-^{13}C]glucose, no significant differences in labelling were observed in synaptosomes (Figure 4(e)). Also in cultured neurons, the labelling patterns derived during second turn TCA cycle metabolism were not different in GDH KO neurons compared to control, while the glutamate M + 4 and aspartate M + 3 labelling was significantly increased (Figure 4(f)). Cycling ratios as measurement of the TCA cycling activity were calculated to investigate if the TCA cycle activity might be influenced by the absence of GDH. No significant differences in the cycling ratios were observed in synaptosomes (Figure 4(g)) or cultured neurons (Figure 4(h)). Furthermore, no difference in the total amount of glutamate was observed in GDH KO synaptosomes (control: 68.5 ± 3.0 nmol/mg protein; GDH KO: 81.5 ± 9.0 nmol/mg protein) and in cultured neurons (control: 142.8 ± 37.8 nmol/mg protein; GDH KO: 194.2 ± 47.7 nmol/mg protein).

Glutamine metabolism in the presence of glucose is not affected by the lack of GDH expression

Glutamine metabolism was investigated in the presence of glucose in GDH KO synaptosomes in order to assess the contribution of GDH to glutamine metabolism under conditions of abundant energy substrate availability. The total amounts of glutamine and glutamine M + 5 were not changed by the absence or presence of GDH in synaptosomes (Figure 5(a)) and were similar to values reported before.[15] No significant changes in the amounts of glutamate M + 5, glutamate M + 3, aspartate M + 4 and aspartate M + 2 were observed (Figure 5(b)). In addition, the percent labelling in the direct (Figure 5(c)) and the first turn of TCA cycle (Figure 5(d)) derived metabolites were not changed in the presence of glucose in GDH KO synaptosomes compared to control synaptosomes. Thus, the changes previously observed in glutamine metabolism in GDH KO synaptosomes were abolished in presence of glucose.

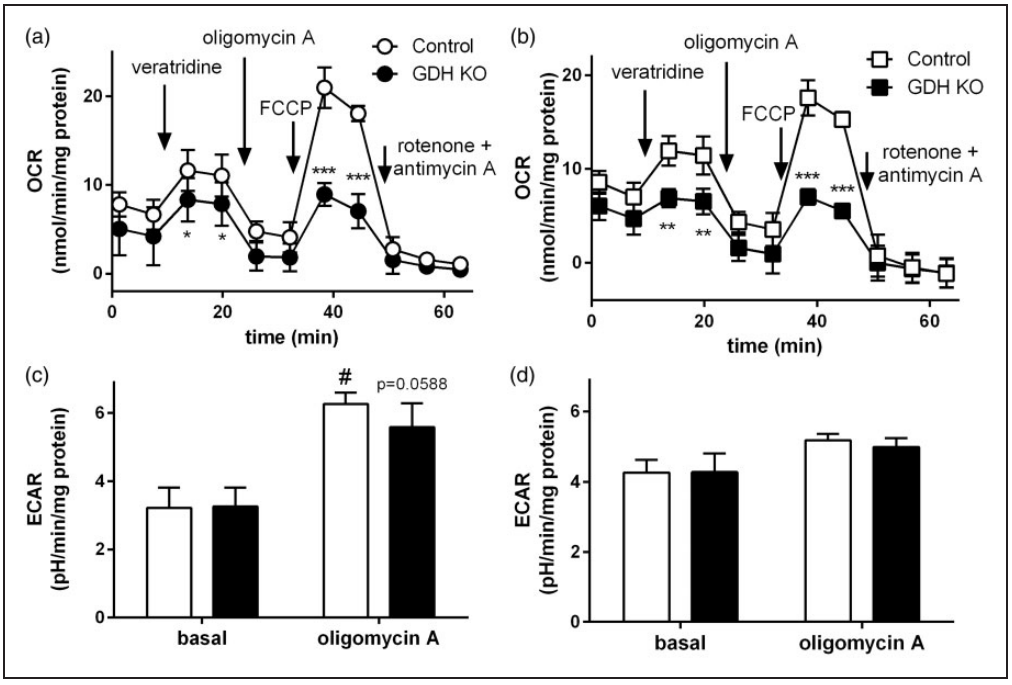

Figure 6. Respiration (OCR) and lactate release (ECAR) of GDH KO synaptosomes. Synaptosomal OCR was monitored in control (white) and GDH KO synaptosomes (black) in the presence of glucose alone (a) or glucose + glutamine (b). Veratridine (5 μM), oligomycin A (12 μM), FCCP (4 μM), and rotenone (2 μM) + antimycin A (2 μM; all final concentrations) were added at the time points indicated by the arrows. Panels (c) and (d) show the basal and oligomycin A-dependent ECAR as average of the 2 time points of the time-dependent measurement of ECAR in control and GDH KO synaptosomes (time dependency not shown) in the presence of glucose alone (c) or glucose + glutamine (d). ($n = 3$ independently prepared synaptosome preparations per condition.)

Increase of the aspartate/glutamate ratio upon glucose withdrawal is GDH dependent

The ratio of aspartate/glutamate of synaptosomes was calculated, because the levels of these two amino acids are connected by the high AAT activity and may indicate operation of the truncated TCA cycle.[9] In the presence of glutamine and glucose the aspartate/glutamate ratio was significantly lower ($p = 0.0019$) in GDH KO synaptosomes (0.35 ± 0.03) compared to control (0.50 ± 0.02). In control synaptosomes, glucose withdrawal caused a significant increase in this ratio (0.80 ± 0.04; $p = 0.000008$), whereas it (0.40 ± 0.10) was not significantly elevated in GDH KO synaptosomes.

Impaired maximal respiration in GDH KO synaptosomes

The ADP-dependent respiration in isolated brain mitochondria obtained from GDH KO mice was significantly decreased when fuelled by glutamate, while it was unaffected when fuelled by pyruvate (Figure 1(b) and (c)). This may be in line with the fact that [U-^{13}C]glutamine metabolism and not [U-^{13}C]glucose metabolism was affected by the lack of GDH expression in synaptosomes. The oxidative deamination of glutamate catalyzed by GDH is accompanied by a reduction of NAD^+ to NADH, thereby directly supporting respiration and ATP production. To investigate the direct effect of GDH on respiration we measured oxygen consumption in synaptosomes fuelled by glucose in the absence and presence of glutamine.[21] The basal respiration was comparable in GDH KO and control synaptosomes in the presence or absence of glutamine (Figure 6(a) and (b)). To test if GDH KO synaptosomes are able to increase respiration upon elevated energy demand, neuronal stimulation was simulated by applying veratridine, a compound inhibiting the closure of Na^+ channels thereby increasing the energy demand[28] and respiration[21,29] in synaptosomes. As expected, stimulation of synaptosomes with veratridine significantly increased the respiration; however, this elevation was lower in GDH KO synaptosomes in the absence and presence of glutamine (Figure 6(a) and (b)). Uncoupling of the mitochondrial respiration by FCCP increased the respiration as expected. However, the response was significantly lower in GDH KO synaptosomes, independent of the presence of glutamine. The injection of rotenone + antimycin

A decreased the synaptosomal respiration almost completely revealing that only mitochondrial respiration contributes to the observed OCR (Figure 6(a) and (b)). Calculation of the maximal and spare respiratory capacity demonstrated that GDH KO synaptosomes have a significantly lower maximal respiration ($44\% \pm 6\%$ of control; $p = 0.0231$) and lower spare respiratory capacity ($24\% \pm 11\%$ of control; $p = 0.0500$) in the presence of glucose (Figure 6(a)). Also in the additional presence of glutamine, the maximal respiration was significantly lower with $43\% \pm 8\%$ ($p = 0.0385$) in GDH KO synaptosomes compared to control (Figure 6(b)).

Since a slightly increased labelling of lactate M + 3 from [U-^{13}C]glucose was observed in GDH KO synaptosomes, the ECAR was analyzed from GDH KO and control synaptosomes to investigate differences in glycolytic activity by proton coupled lactate release. The basal ECAR in the presence of glucose in the absence or presence of glutamine were comparable in GDH KO and control synaptosomes (Figure 6(c) and (d)). In the presence of glucose as the only substrate, injection of oligomycin significantly increased ECAR and this increase was slightly lower, although not significant, in GDH KO synaptosomes (Figure 6(c)). In the presence of glucose + glutamine, the injection of oligomycin only slightly increased ECAR and no difference was observed between GDH KO and control synaptosomes (Figure 6(d)).

Discussion

The main fuel for the brain is systemically derived glucose. The glucose-derived carbon skeleton is in equilibrium with several metabolic pools as part of the oxidation and among these pools are glutamate and glutamine. These metabolic pools (e.g. glutamate or glutamine) can subsequently be used as substrate to replenish TCA cycle intermediates. In addition, glutamate is an important energy substrate in the brain for the regulation of the body energy homeostasis.[10] In vitro, substrates such as glutamate and glutamine supplied in the incubation medium can be used by cultured neurons or astrocytes as metabolic fuels in the presence or absence of glucose. Several studies have investigated the role of GDH for amino acid and energy metabolism in astrocytes[7–10] and the role of GDH in astrocytes with respect to the glutamine–glutamate cycle as recently been reviewed.[30] However, little is known about the physiological role of GDH in neurons and its role during stimulation. The present study aimed to fill this gap of knowledge. The absence of GDH in brain mitochondria of the GDH KO mouse was confirmed by protein expression and enzyme activity measurements.[11,20] The conversion of glutamate to α-ketoglutarate catalyzed by AAT simultaneously synthesizing aspartate from oxaloacetate formed via the TCA cycle from α-ketoglutarate (Figure 7(a), control neuron) is named the truncated TCA cycle. The AAT catalyzed reaction can potentially to some extent substitute for the GDH catalyzed reaction using the truncated TCA cycle which is experimentally observed by an increased cellular aspartate content at the expense of glutamate, as reported for astrocytes.[7,9] The truncated TCA cycle has been reported in cultured neurons[13–15] and synaptosomes during glucose deprivation[17,31] (Figure 7(a), control neuron) and it provides energy from partial glutamate oxidation during limited acetyl-CoA availability. The increased aspartate/glutamate ratio, upon glucose withdrawal in the presence of glutamine in control synaptosomes, was not observed in GDH KO synaptosomes. This suggests that GDH KO neurons are unable to increase the activity of the truncated TCA cycle to metabolize glutamine upon glucose withdrawal (Figure 7(a), GDH KO neuron). The lack of an elevated truncated TCA cycle activity may be caused by different reasons, for example by a lower activity of AAT. We did not observe differences in the expression and enzyme activity of AAT, suggesting that AAT activity may not be a limiting factor. AAT activity has been reported to depend on the formation of multienzyme complexes with GDH.[27] Thus, the actual AAT activity may still be lower in the microenvironment lacking GDH compared to the condition in a test tube. In addition, the AAT activity may change during low energy availability, because the AAT activity is dependent on the phosphate concentration.[1] In cultured cerebellar granule cells, stimulation by applying 26 mM KCl increased the mitochondrial AAT activity, but this observation has been suggested to be due to protein synthesis not increased activity of the enzyme.[32] We observed a significantly lower respiration in GDH KO mitochondria fuelled by glutamate, which supports the need of GDH in order for AAT to function at an optimum. Our in vitro data show that GDH is an important enzyme in order for neurons to use glutamate and thus glutamine-derived carbon for mitochondrial respiration. Indeed, during glucose deprivation, elevations in ADP activate GDH mediated metabolism.[27] This may suggest that the GDH catalyzed reaction increases the pool of TCA cycle intermediates particularly during low energy conditions. An increased pool of TCA cycle intermediates facilitates a higher TCA cycle activity producing more substrate for the respiration and ATP production. Thus, GDH is a key enzyme in order to increase neuronal TCA cycle metabolism upon limited availability of energy substrate, such as hypoglycemia, likely causing an elevated ADP concentration (Figure 7(a)).

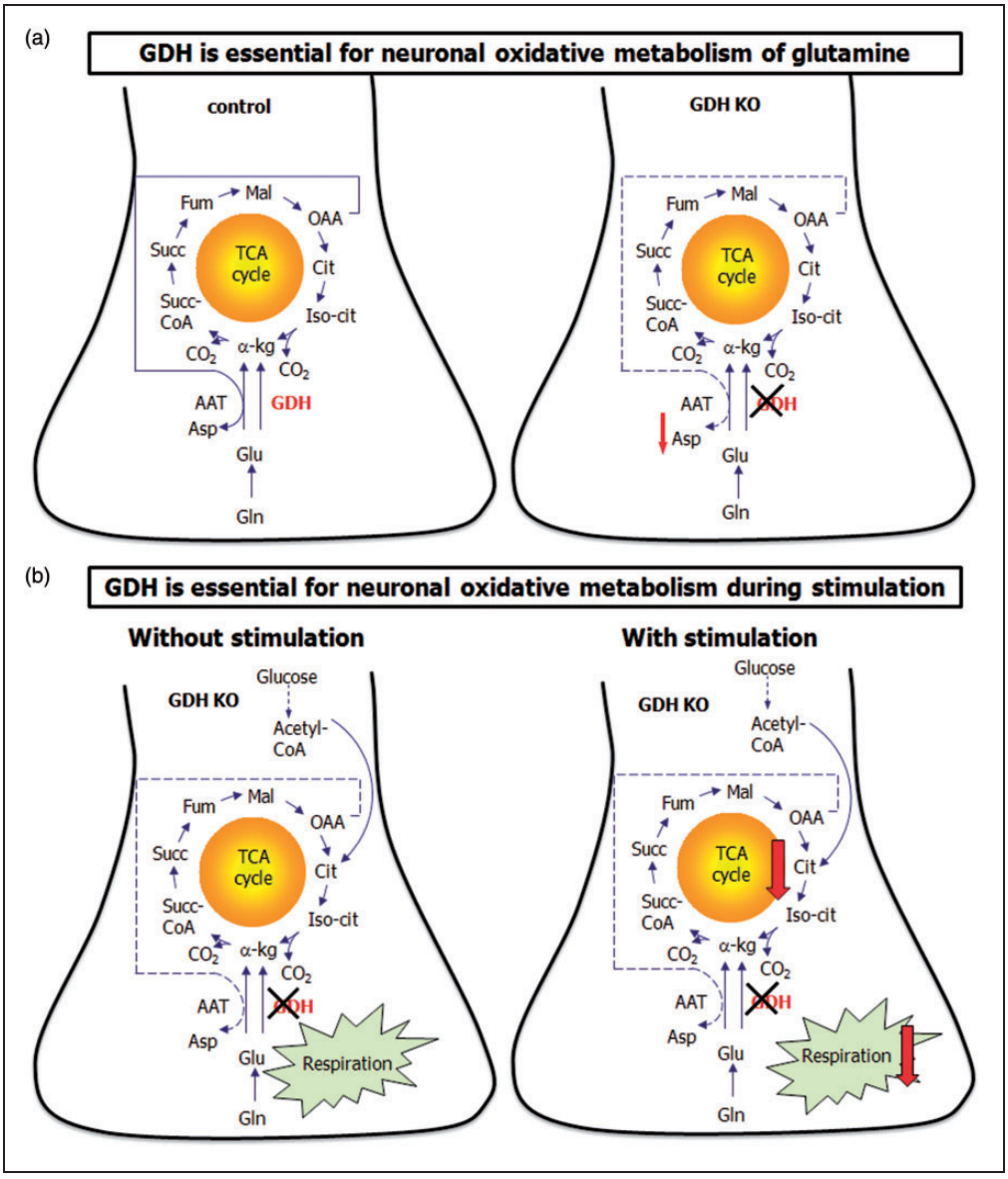

Figure 7. Metabolic pathways affected by GDH KO in neurons. In the presence of GDH neurons metabolize glutamine by the truncated TCA cycle in the absence of glucose (a, control). GDH KO neurons metabolize glutamine, but are not able to use the truncated TCA cycle upon glucose deprivation as shown by deceased aspartate content (a, GDH KO). GDH KO neurons metabolize glucose and respire in the presence of glucose ± glutamine comparable to control neurons (b, without stimulation). However, upon stimulation (e.g. veratridine or FCCP), GDH KO neurons are not able to respond with an increased respiration (b, with stimulation).

Glutaminase is expressed in neurons and two isoenzymes have been observed, one in mitochondria and one in the nucleus.[33] The function of the nucleus glutaminase remains to be elucidated. The mitochondrial isoform provides glutamate from glutamine either as neurotransmitter or as carbon source for TCA cycle oxidation and it is the most important glutamine-utilizing enzyme in neurons.[34] Glutaminase catalyzes the hydrolytic deamidation of glutamine to glutamate and ammonium. This glutamate can subsequently be used as neurotransmitter or enter the TCA cycle for oxidation of the carbon skeleton. Metabolism of the resulting ammonium needs to match the generated ammonium, because high levels of ammonium are neurotoxic. The ammonium has been proposed to be fixed in amino acids such as alanine and branched-chain amino acids and subsequently be transferred to astrocytes. The ammonium metabolism in relation to glutamate metabolism[6,30] and nitrogen homeostasis has been reviewed recently.[6] In addition, glutaminase has been suggested to be important for neuronal differentiation and survival.[33]

It may be speculated that GDH-deficient neurons compensate a hampered mitochondrial function by elevated glycolytic activity. However, glycolysis was not increased, which was apparent from the lack of an elevated lactate M + 3 and alanine M + 3 labelling from [U-^{13}C]glucose or extracellular lactate amounts (data not shown). Furthermore, no significant differences in the glycolytic acidification rate of GDH KO synaptosomes were noticed after inhibition of mitochondrial ATP synthesis with oligomycin, indicating no alterations in glycolysis. It may be noted that the absence of an activated glycolysis could be due to the time point chosen in this study, although the fact that neurons do not increase glycolysis during augmented energy demand has been reported before.[35] The basal respiration fuelled by glucose and pyruvate in synaptosomes and mitochondria, respectively, was not affected by the lack of GDH activity (Figure 7(b), without stimulation). This observation is supported by the absence of any effect of GDH in cycling ratios obtained from metabolism of [U-^{13}C]glucose in neurons and synaptosomes. Thus, it may be concluded that GDH plays a minor role to maintain basal oxidative metabolism of glucose in neurons without an elevated ATP demand. In addition, oxidative glutamine metabolism was maintained in GDH deficient neurons in the presence of glucose in our in vitro experiments. However, it may be speculated that the lower aspartate/glutamate ratio in the combined presence of glutamine and glucose in GDH KO synaptosomes might reflect a lack of TCA cycle intermediates. A low amount of TCA cycle intermediates may hamper a potential increase in oxidative glucose metabolism during stimulation (Figure 7(b), with stimulation).

In vivo, glucose oxidation has been coupled to the glutamate–glutamine cycle.[36] In anesthetized rats, an increased neuronal oxidative metabolism and activity of the glutamate–glutamine cycle was observed upon hind and fore paw stimulation.[36] In the present study, the physiological stimulation of neurons was simulated by applying veratridine to the synaptosomes, which increases respiration in synaptosomes[21,29] and in mouse cortical neurons.[37] The augmented energy demand caused by veratridine caused a significantly elevated respiration in synaptosomes lacking GDH that was lower compared to the increase observed in control synaptosomes suggesting that GDH is essential for neurons in order to increase the TCA cycle capacity (Figure 7(b), with stimulation). Furthermore, it implies that the TCA cycle is functional in the absence of GDH under basal conditions and intact glucose metabolism (Figure 7(a), GDH KO neurons). Uncoupling induced by FCCP caused the expected increase in respiration, however, it was significantly lower in GDH KO synaptosomes (Figure 7(b), GDH KO neuron) compared to control. This may also be due to a hampered TCA cycle capacity when GDH is not operative. Besides the importance of GDH to support elevations of TCA cycle capacity, GDH supports the respiratory chain directly with substrate in the form of NADH. The importance of the GDH reaction for ATP production is recognized and was evident from experiments using GDH knock out immortalized human proximal tubule epithelial cells.[38] Thus, GDH is highly important for energy generation under conditions of elevated energy requirements, not only in neurons.

Humans express the GDH isoform human GDH2 (hGDH2). A recent study suggested hGDH2 expression in mitochondria of pre-synaptic terminals.[39] Expression of hGDH2 in neurons might enable these cells to utilize glutamate for ATP production and thus spare glucose as substrate or to strengthen excitatory synaptic transmission by enhancing the formation of glutamate.[39] Augmented expression of GDH in mouse cortical neurons in vivo has been shown to increase pre-synaptic release of glutamate.[40] Elevated glutamate release augments excitatory neurotransmission and requires mitochondria for energy production in nerve terminals.[41] Isolated brain mitochondria from GDH KO mice exhibited a significantly reduced respiration in the presence of glutamate as substrate suggesting that AAT alone may not be able to maintain mitochondrial respiration in the time frame employed in the present study. In isolated mitochondria, the maximal respiration (induced by uncoupling with FCCP) is not different in the absence or presence of GDH. As the mitochondria respire on pyruvate as substrate, the pyruvate dehydrogenase reaction may provide sufficient NADH for maximal respiration under the present experimental conditions. Oxidative metabolism of [U-^{13}C]glutamine in synaptosomes was more affected by the lack of functional GDH than that in cultured neurons. Synaptosomes may exhibit a higher energy requirement compared to cultured neurons. Neuron cultures have different subtypes of mitochondria, and therefore may be slightly better in handling glutamine as substrate in the absence of GDH in vitro. This view is consistent with the existence of different metabolite pools, which are not in direct exchange (compartmentation) in neurons.[42]

Funding

The author(s) disclosed receipt of the following financial support for the research, authorship, and/or publication of this article: Michaela C Hohnholt would like to thank the 'Deutsche Forschungsförderung (DFG)' for financial support (HO 5204/2-1). Helle S Waagepetersen thanks the Carlsberg Foundation for financial support (grant number 108559100).

Acknowledgement

We would like to thank Heidi M Nielsen and Catia CG Andersen for excellent technical assistance.

Declaration of conflicting interests

The author(s) declared no potential conflicts of interest with respect to the research, authorship, and/or publication of this article.

Authors' contributions

MCH and HSW designed research; VHA performed the synaptosomes Seahorse experiments and the GDH and AAT enzyme activity assays, JVA performed the mitochondria Seahorse experiments and SKC performed the Western blots of GDH and AAT. MCH performed all ^{13}C-labelling experiments and analyzed the data; MCH and HSW wrote the manuscript; MK and PM generated the Cns-*Glud1*$^{-/-}$ mice. All authors contributed to the discussion and final draft of the manuscript.

References

1. McKenna MC. The glutamate-glutamine cycle is not stoichiometric: fates of glutamate in brain. *J Neurosci Res* 2007; 85: 3347–3358.
2. Kim K, Lee SG, Kegelman TP, et al. Role of excitatory amino acid transporter-2 (EAAT2) and glutamate in neurodegeneration: opportunities for developing novel therapeutics. *J Cell Physiol* 2011; 226: 2484–2493.
3. Schmitt A and Kugler P. Cellular and regional expression of glutamate dehydrogenase in the rat nervous system: non-radioactive in situ hybridization and comparative immunocytochemistry. *Neuroscience* 1999; 92: 293–308.
4. Rothe F, Brosz M and Storm-Mathisen J. Quantitative ultrastructural localization of glutamate dehydrogenase in the rat cerebellar cortex. *Neuroscience* 1994; 62: 1133–1146.
5. Erecinska M and Silver IA. Metabolism and role of glutamate in mammalian brain. *Prog Neurobiol* 1990; 35: 245–296.
6. Cooper AJ and Jeitner TM. Central role of glutamate metabolism in the maintenance of nitrogen homeostasis in normal and hyperammonemic brain. *Biomolecules* 2016; 6: E16.
7. Skytt DM, Klawonn AM, Stridh MH, et al. siRNA knock down of glutamate dehydrogenase in astrocytes affects glutamate metabolism leading to extensive accumulation of the neuroactive amino acids glutamate and aspartate. *Neurochem Int* 2012; 61: 490–497.
8. Pajecka K, Nissen JD, Stridh MH, et al. Glucose replaces glutamate as energy substrate to fuel glutamate uptake in glutamate dehydrogenase-deficient astrocytes. *J Neurosci Res* 2015; 93: 1093–1100.
9. Nissen JD, Pajecka K, Stridh MH, et al. Dysfunctional TCA-cycle metabolism in glutamate dehydrogenase deficient astrocytes. *Glia* 2015; 63: 2313–2326.
10. Karaca M, Frigerio F, Migrenne S, et al. GDH-dependent glutamate oxidation in the brain dictates peripheral energy substrate distribution. *Cell Rep* 2015; 13: 365–375.
11. Frigerio F, Karaca M, De Roo M, et al. Deletion of glutamate dehydrogenase 1 (Glud1) in the central nervous system affects glutamate handling without altering synaptic transmission. *J Neurochem* 2012; 123: 342–348.
12. Zaganas I, Waagepetersen HS, Georgopoulos P, et al. Differential expression of glutamate dehydrogenase in cultured neurons and astrocytes from mouse cerebellum and cerebral cortex. *J Neurosci Res* 2001; 66: 909–913.
13. Olstad E, Qu H and Sonnewald U. Glutamate is preferred over glutamine for intermediary metabolism in cultured cerebellar neurons. *J Cereb Blood Flow Metab* 2007; 27: 811–820.
14. Waagepetersen HS, Qu H, Sonnewald U, et al. Role of glutamine and neuronal glutamate uptake in glutamate homeostasis and synthesis during vesicular release in cultured glutamatergic neurons. *Neurochem Int* 2005; 47: 92–102.
15. Sonnewald U and McKenna M. Metabolic compartmentation in cortical synaptosomes: influence of glucose and preferential incorporation of endogenous glutamate into GABA. *Neurochem Res* 2002; 27: 43–50.
16. McKenna MC, Tildon JT, Stevenson JH, et al. Regulation of energy metabolism in synaptic terminals and cultured rat brain astrocytes: differences revealed using aminooxyacetate. *Dev Neurosci* 1993; 15: 320–329.
17. Yudkoff M, Nelson D, Daikhin Y, et al. Tricarboxylic acid cycle in rat brain synaptosomes. Fluxes and interactions with aspartate aminotransferase and malate/aspartate shuttle. *J Biol Chem* 1994; 269: 27414–27420.
18. Su TZ, Campbell GW and Oxender DL. Glutamine transport in cerebellar granule cells in culture. *Brain Res* 1997; 757: 69–78.
19. Dolinska M, Zablocka B, Sonnewald U, et al. Glutamine uptake and expression of mRNA's of glutamine transporting proteins in mouse cerebellar and cerebral cortical astrocytes and neurons. *Neurochem Int* 2004; 44: 75–81.
20. Karaca M and Maechler P. Development of mice with brain-specific deletion of floxed glud1 (glutamate dehydrogenase 1) using cre recombinase driven by the nestin promoter. *Neurochem Res* 2014; 39: 456–459.
21. Hohnholt MC, Andersen VH, Bak LK, et al. Glucose, lactate and glutamine but not glutamate support depolarization-induced increased respiration in isolated nerve terminals. *Neurochem Res* 2016; 42: 191–201.
22. Bak LK, Johansen ML, Schousboe A, et al. Valine but not leucine or isoleucine supports neurotransmitter glutamate synthesis during synaptic activity in cultured cerebellar neurons. *J Neurosci Res* 2012; 90: 1768–1775.
23. Walls A, Bak L, Sonnewald U, et al. Metabolic mapping of astrocytes and neurons in culture using stable isotopes and gas chromatography-mass spectrometry (GC-MS). In: Hirrlinger J and Waagepetersen HS (eds) *Brain energy metabolism*, Neuromethods ed. New York: Springer, 2014, pp.73–105.
24. Lowry OH, Rosebrough NJ, Farr AL, et al. Protein measurement with the Folin phenol reagent. *J Biol Chem* 1951; 193: 265–275.
25. Andersen JV, Christensen SK, Aldana BI, et al. Alterations in cerebral cortical glucose and glutamine metabolism precedes amyloid plaques in the APPswe/

PSEN1dE9 mouse model of Alzheimer's disease. *Neurochem Res* 2016; 42: 1589–1598.
26. Bak LK, Obel LF, Walls AB, et al. Novel model of neuronal bioenergetics: postsynaptic utilization of glucose but not lactate correlates positively with Ca^{2+} signalling in cultured mouse glutamatergic neurons. *ASN Neuro* 2012; 4: e83.
27. McKenna MC, Stevenson JH, Huang X, et al. Differential distribution of the enzymes glutamate dehydrogenase and aspartate aminotransferase in cortical synaptic mitochondria contributes to metabolic compartmentation in cortical synaptic terminals. *Neurochem Int* 2000; 37: 229–241.
28. Rose CR and Ransom BR. Regulation of intracellular sodium in cultured rat hippocampal neurones. *J Physiol* 1997; 499(Pt 3): 573–587.
29. Choi SW, Gerencser AA and Nicholls DG. Bioenergetic analysis of isolated cerebrocortical nerve terminals on a microgram scale: spare respiratory capacity and stochastic mitochondrial failure. *J Neurochem* 2009; 109: 1179–1191.
30. Hertz L and Rothman DL. Glutamine-glutamate cycle flux is similar in cultured astrocytes and brain and both glutamate production and oxidation are mainly catalyzed by aspartate aminotransferase. *Biology (Basel)* 2017; 6: E17.
31. Yudkoff M, Zaleska MM, Nissim I, et al. Neuronal glutamine utilization: pathways of nitrogen transfer studied with [^{15}N]glutamine. *J Neurochem* 1989; 53: 632–640.
32. Caballero-Benitez A, Alavez S, Uribe RM, et al. Regulation of glutamate-synthesizing enzymes by NMDA and potassium in cerebellar granule cells. *Eur J Neurosci* 2004; 19: 2030–2038.
33. Campos-Sandoval JA, Martin-Rufian M, Cardona C, et al. Glutaminases in brain: multiple isoforms for many purposes. *Neurochem Int* 2015; 88: 1–5.
34. Marquez J, Campos-Sandoval JA, Penalver A, et al. Glutamate and brain glutaminases in drug addiction. *Neurochem Res* 2017; 42: 846–857.
35. Bolanos JP. Bioenergetics and redox adaptations of astrocytes to neuronal activity. *J Neurochem* 2016; 139(Suppl. 2): 115–125.
36. Sonnay S, Duarte JM, Just N, et al. Compartmentalised energy metabolism supporting glutamatergic neurotransmission in response to increased activity in the rat cerebral cortex: a 13C MRS study in vivo at 14.1 T. *J Cereb Blood Flow Metab* 2016; 36: 928–940.
37. Llorente-Folch I, Rueda CB, Amigo I, et al. Calcium-regulation of mitochondrial respiration maintains ATP homeostasis and requires ARALAR/AGC1-malate aspartate shuttle in intact cortical neurons. *J Neurosci* 2013; 33: 13957–13971.
38. Romanov V, Whyard T, Bonala R, et al. Glutamate dehydrogenase requirement for apoptosis induced by aristolochic acid in renal tubular epithelial cells. *Apoptosis* 2011; 16: 1217–1228.
39. Spanaki C, Kotzamani D, Kleopa K, et al. Evolution of GLUD2 glutamate dehydrogenase allows expression in human cortical neurons. *Mol Neurobiol* 2016; 53: 5140–5148.
40. Bao X, Pal R, Hascup KN, et al. Transgenic expression of Glud1 (glutamate dehydrogenase 1) in neurons: in vivo model of enhanced glutamate release, altered synaptic plasticity, and selective neuronal vulnerability. *J Neurosci* 2009; 29: 13929–13944.
41. Verstreken P, Ly CV, Venken KJ, et al. Synaptic mitochondria are critical for mobilization of reserve pool vesicles at *Drosophila* neuromuscular junctions. *Neuron* 2005; 47: 365–378.
42. Waagepetersen HS, Sonnewald U, Larsson OM, et al. Compartmentation of TCA cycle metabolism in cultured neocortical neurons revealed by ^{13}C MR spectroscopy. *Neurochem Int* 2000; 36: 349–358.